JOURNAL OF GEOPHYSICAL RESEARCH, VOL. 105, NO. D15, PAGES 19,927–19,940, AUGUST 16, 2000

Modeled impact of cirrus cloud increases along aircraft flight paths

D. Rind, P. Lonergan,[1] and K. Shah[2]

Goddard Space Flight Center, Institute for Space Studies, New York

Abstract. The potential climate impact of contrails and alterations in the lifetime of background cirrus due to subsonic aircraft water and aerosol emissions has been investigated in a set of experiments using the GISS GCM connected to a q-flux ocean. Cirrus clouds at a height of 12–15 km, with an optical thickness of 0.33, were input to the model "x" percentage of clear-sky occasions along subsonic aircraft flight paths. The percentage x is varied from 0.05 to 6%. Two types of experiments were performed: one with the percentage of cirrus cloud increase independent of flight density along the flight paths, the other with the percentage related to the density of fuel expenditure. The overall climate impact was similar with the two approaches, due to the feedbacks of the climate system. Fifty years were run for each of the eight experiments, with the following conclusions based on the stable results from years 31–50. The equilibrium global mean response shows that altering high-level clouds by 1% changes the global mean temperature by 0.43°C. The global temperature response is highly linear (linear correlation coefficient of 0.996) for high cloud cover changes between 0.1 and 5%. The warming is amplified in the Northern Hemisphere, more so with greater cloud cover change. The temperature effect maximizes around 10 km, more so as the overall warming increases (warming greater than 4°C occurs there with a 4.8% increase in upper level clouds). The surface temperature response is dominated by the feedbacks and shows little geographic relationship to the high cloud input outside of the hemispheric difference. Considering whether these effects would be observable, changing upper level cloud cover by as little as 0.4% produces warming greater than 2 standard deviations in the microwave sounding unit (MSU) channels 4, 2, and 2r (although the effect would be most noticeable in the upper troposphere channel 3 were standard deviations available). Given estimates of current aircraft impacts, this would require some increase relative to present-day effects, but a signal should be clear given the projections for 2050 aircraft. In comparison to increased CO_2 experiments, in these runs the Northern Hemisphere clearly warms more relative to the Southern Hemisphere, and warming due to cloud height changes exceeds that due to the water vapor feedback. Despite the simplified nature of these experiments, the results emphasize the sensitivity of the modeled climate to high-level cloud cover changes and thus the potential ability of aircraft to influence climate by altering clouds in the upper troposphere.

1. Introduction

A major uncertainty associated with the impact of aircraft on climate concerns how subsonic aircraft may be influencing upper level cloud cover. Contrails are the obvious aircraft effects, visible in the clear sky. Less obvious are the impacts on natural cirrus, both in terms of extending their lifetime and in altering their optical thickness.

Aircraft may impact cirrus clouds through the process of heterogeneous nucleation, i.e., the triggering of liquid freezing by a solid particle or surface. This takes place in air that is supersaturated with respect to ice [*Brewer*, 1946] but not supersaturated sufficiently for homogeneous nucleation to occur [*Heymsfield et al*., 1998]. It is estimated that air masses sufficiently cold and humid to allow for persistent contrails may cover an area of Europe and the United States amounting to 10–20% [*Mannstein et al*., 1999; *Travis and Changnon*, 1997]. The global mean value is estimated to be 16% coverage [*Sausen et al*., 1998; *International Panel on Climate Change* (*IPCC*), 1999].

The vertical motions and small-scale temperature and humidity fluctuations associated with aircraft emissions cannot be directly simulated in general circulation models (GCMs). *Rind et al*. [1996] found that even a factor of 3.5 times increase in aircraft water vapor emissions over present-day values failed to produce a change in high-level cloud cover. It has been observed that the ice water content of new contrails increases with time to exceed the amount of water emitted by the aircraft by more than 2 orders of magnitude. This is because while aircraft initially form contrails with extreme supersaturation locally, the subsequent development depends on the ambient water vapor [*Knollenberg*, 1972]. Hence parameterizations are

[1]Science Systems and Applications, Inc., New York.

[2]Center for Climate System Research, Columbia University, New York.

Paper number 1999JD901160.
0148-0227/00/1999JD901160$09.00

necessary when using large-scale models, as has been suggested by *Sausen et al*. [1998].

The frequency of linear persistent contrails (as distinguished from the effect of contrails on naturally occurring cirrus, or on cirrus that form initially as contrails) has been estimated at a few locations. Across the United States the frequency is estimated at 9% of the time [*Minnis et al*., 1997]; the results also implied that contrails in this region are limited mainly by the number of aircraft flights and not by atmospheric conditions. However, in both the United States and the former Soviet Union, contrails maximize in winter or in spring, with a minimum in summer, implying an ambient atmospheric influence as well [*Minnis et al*., 1997; *Sassen*, 1997; *Mazin*, 1996].

Considering the area of coverage, using advanced very high resolution radiometer (AVHRR) images, a mean contrail cover of 0.5% has been found for the Northeast Atlantic and Europe [*Bakan et al*., 1994]. A diurnal variation occurs, with coverage at night over Europe one-third that of the noontime value. Considering aircraft emissions and flight paths and normalizing to produce a value of 0.5% in the European/Atlantic region, the global average contrail coverage has been estimated at about 0.1%, with a maximum of 5% over the eastern United States [*Sausen et al*., 1998]. A value up to 0.2% cannot be ruled out, because the scaling is based solely on observed line-shaped contrail cover. Various studies estimate that cirrus clouds have increased, relative to those values in nonair traffic regions, by ~1.5%/decade since 1970 in regions with contrail cover greater than 0.5%. This is equivalent to an increase since the beginning of the jet aircraft era (end of the 1960s) of about 0.3% cover of the Earth's surface. As this cloud cover change could have been affected by other processes (e.g., global warming), it probably represents an upper bound for aviation-induced cloudiness, although these other changes could also have masked a greater aircraft influence. *Boucher* [1999] emphasizes the good correlation between increasing fuel consumption from the early 1980s to the early 1990s and the observation of increased cirrus frequency.

Estimates of the radiative impact of linear persistent contrails, with an optical thickness of 0.3–0.5 and a global coverage of 0.1%, result in a net forcing of ~0.02 W m^{-2}, a value that may differ from the real value by a factor of 3 to 4 [*IPCC*, 1999]. The effect on cirrus in general, associated with a 0.2% increase, would be about 0.04 W m^{-2}. Estimates for 2050 are that the forcing due to linear persistent contrails may rise by a factor of 5 (hence faster than the factor of 3 for fuel usage) to a value close to 0.1 W m^{-2} and, for cirrus in general, increase by a factor of 4 to 0.16 W m^{-2}. The future projections have a large range, from as little as 0.03 to as high as 0.4 W m^{-2}, related to various emission growth and engine efficiency scenarios [*IPCC*, 1999].

There have been a few previous studies to investigate the effect of contrails on climate. *Ponater et al*. [1996] incremented existing upper level cloud cover (320–150 mbar) by 2, 5, and 10%. Only the 10% case produced a significant effect on the global top of the atmosphere net radiation, reducing it by 1 W m^{-2}. The surface air temperature response was minimized by the use of unchanging sea surface temperatures; nevertheless, surface air temperature changes of 1°K resulted in northern midlatitudes with a 5% additional cirrus cloud cover in the main traffic regions. This study is the first to our knowledge to explore the impacts of contrails in an atmospheric GCM coupled to an interactive ocean.

2. Experiments

Sausen et al. [1998] suggest an approach for determining the likelihood of contrail formation based on the Schmidt-Appleman criterion, in which contrails occur when the ambient air temperature is cooler than some threshold value, which depends on flight level, ambient humidity, and aircraft propulsion efficiency. A typical value is −40°C. The persistence of contrails depends on the air being supersaturated with respect to ice but not with respect to water. As noted above, persistent contrails are not basically formed from the water emitted by aircraft; rather the aircraft emissions trigger the formation of additional clouds from natural water vapor present in the atmosphere.

Difficulties exist in employing parameterizations such as that described above. A parameter of great importance is the ambient humidity; most models have difficulty producing realistic values in the upper troposphere, although it is also somewhat uncertain what the proper values are. Establishing local supersaturation from aircraft water vapor emissions is not possible in GCMs, in which the effect of realistic water vapor emissions is diluted by being spread over large model grid boxes; hence *Rind et al*. [1996] found no effect on upper level clouds with current aircraft water vapor sources. Altering the persistent cloud cover, as was done by *Ponater et al*. [1996], is of no use if the model fails to produce the proper cloud cover, another major uncertainty. Since additional uncertainty exists concerning what the real aviation impact is, whatever parameterization is chosen may be hard to validate in terms of a realistic forcing.

In the light of these considerations we chose to perform a relatively simple set of experiments. The Goddard Institute for Space Studies (GISS) model has no fractional cloud coverage, the grid box is either completely cloud-covered or clear, and the fractional cloud coverage is simulated by a temporal mean [*Hansen et al*., 1983]. With the middle-atmosphere version of this model, the GISS Global Climate Middle-Atmosphere Model (GCMAM) [*Rind et al*., 1988], additional cirrus clouds at a height of 12 km (at high latitudes) to 14 km (low latitudes) were input to the model "x" percentage of clear-sky occasions along subsonic aircraft flight paths, where x is varied from 0.05 to 5%; that is, 100 $(1 - x)$ time steps without clouds are followed by 100× (previously clear sky) time steps with cloud cover. For example, considering the 1% experiment, after every 99 clear-sky occasions at a particular location along a flight path, a cirrus cloud is inserted at the next clear-sky occasion. The counting then begins again. For the largest increase (5%), after 95 cloud-free calculations, a cloud is inserted for the next five cloud-free calculations, before new counting is initiated. A list of these experiments is given in Table 1.

The altitude chosen in the model is at a temperature below −40°C, hence it meets a main criterion noted above. The relative humidity is undersaturated with respect to water; however, it is only occasionally supersaturated with respect to ice. Given the uncertainties in the validity of the model in situ water vapor concentrations, as this level best represents the cruising altitude for subsonic aircraft, it is chosen for cloud cover augmentation regardless of its moisture distribution. The optical thickness for the input cirrus cloud is 0.33, similar to the background cirrus, and consistent with observations for persistent contrails [e.g., *Jager et al*., 1998; *Minnis et al*., 1997]. (In fact, the GISS GCM recomputes cloud cover in phase with its new radiation calculation, which occurs every 5 hours. This means that every condition, be it clear sky or cirrus cloud

Table 1. List of Experiments

Experiment	Description
Control	no cirrus cloud insertion
1/200	cirrus cloud insertion in the clear-sky hour after 200 clear-sky hours
1/150	cirrus cloud insertion after 150 clear-sky hours
1/100	cirrus cloud insertion after 100 clear-sky hours
1/99	cirrus cloud insertion after 99 clear-sky hours
1/98	cirrus cloud insertion for the 2 clear-sky hours after 98 clear-sky hours
1/97	cirrus cloud insertion for the 3 clear-sky hours after 97 clear-sky hours
1/96	cirrus cloud insertion for the 4 clear-sky hours after 96 clear-sky hours
1/95	cirrus cloud insertion for the 5 clear-sky hours after 95 clear-sky hours
Scaled	cirrus cloud insertion varying between the insertion procedure for the 1/200 and 1/95 experiments, proportional to flight density

insertion, actually lasts for 5 hours. This does not change the percentage of time that cirrus clouds are inserted but does imply it is persistent contrails or cirrus that are being considered here. Observations by *Sassen* [1997] and others suggest that contrails lasting only up to 1 hour actually have smaller particles than natural cirrus and hence probably have a larger albedo than used here.)

To investigate the sensitivity of the results to details of the specification, two different types of experiments are performed. Most of the runs do not differentiate aircraft flight densities in a grid box; the procedure is used at all locations above a certain minimum flight path density (peak emission values for civil aviation >10 Kg d^{-1} [see *IPCC*, 1999, Figures 9–10]). This approach in effect suggests that the ambient conditions are more important than the number of flights, and since we are not certain about the ambient conditions, we assume no bias in cirrus cloud impact. In one experiment we scale the cirrus cloud input (from 0.05 to 5%) based on the density of the flight paths (dividing regions proportionately between the minimum and the maximum flight path density), in effect assuming that flight density, and not ambient conditions, is the sole determinant. A comparison of the cloud cover insertion distribution from this experiment with a uniform-increase experiment that resulted in a similar global cloud cover change is given in Plates 1a and 1b. The results for the scaled experiment highlight the flight path regions and are in generally good agreement with fuel consumption shown by *Sausen et al*. [1998], for example. Of course, in regions that have a greater frequency of high clouds naturally in the model (not a dominant issue at this level but more frequent in the tropics), fewer opportunities will arise for cloud cover augmentation.

Each experiment is integrated for 50 years with a "q-flux" ocean in which ocean heat transports and mixed layer depths are specified, with sea surface temperatures allowed to change due to net heating imbalances (as in the work of *Rind et al*. [1996]). Results shown are averages for years 31–50, which are stable in all of the experiments. Since the experiment in which a cloud is inserted after 200 cloud-free hours is virtually identical to the control run with no cloud insertion, its results will not be shown below.

3. Results

3.1. Cloud Cover

For comparison with observations presented above and the subsequent discussion, we first show the impact of the cloud insertion on total upper level cloud cover (above 500 mbar). The cloud insertion, as will be shown below, leads to warming below the cloud; this has the effect of stabilizing the atmosphere, and reducing cloud cover somewhat (by 1.5% absolute cloud cover change in each layer between 500 and 200 mbar between the extreme experiments, and 1–2% absolute change overall). Therefore the total impact on high-level cloud cover is slightly less than the cloud addition would imply. Given in Plate 2 are the actual upper level cloud cover changes (above 500 mbar) in the different experiments, along with the global average change. The global and latitudinal-average figures shown below will henceforth refer to the experiments by this impact on upper level cloud cover.

Comparison of Plate 2 with Plate 1 reveals that the effect on upper level cloud cover in the uniform input experiments mimics the extreme Northern Hemisphere bias of the cloud cover input. However, the forced climate change also impacts upper level clouds and produces some differences from the input distribution, discussed further below. The scaled experiment has an overall similar response to the experiment that produced a similar global average change in upper level clouds (1/99 or 1.2%), outside of the localized areas of exaggerated change over the eastern United States, western Europe, and extreme eastern Asia, which more closely follow the cloud cover insertion.

The effect of upper level cloud cover changes of this magnitude on the surface air temperature is given in Figures 1–3 and Plate 3. Figure 1 shows the global mean temperature change, relative to the change in (absolute) high-level cloud cover percentage. The results are strongly linear, although the deviations from linearity result in slightly reduced warming at higher cloud cover values, possibly due to diminishing effects of feedbacks such as sea ice or snow cover; the radiative forcing is approximately linear with cloud cover change, as shown in section 3.3 below. A change in high-level cloud cover of 1% results in an increase in global mean temperature of some 0.43°C. The input cloud cover has a Northern Hemisphere bias, which explains the greater sensitivity of the Northern Hemisphere surface air temperature (as discussed more fully below, in a doubled CO_2 experiment with the same model, as reported by *Rind et al*. [1998], the Southern Hemisphere actually had a slightly greater climate sensitivity). Cirrus cloud cover input along flight paths results in a 40% greater response in the Northern Hemisphere. The asterisks in Figure 1 represent the results from the scaled experiment, and their location indicates the small difference its high cloud cover input makes relative to the uniformly distributed input along the flight paths in the other experiments.

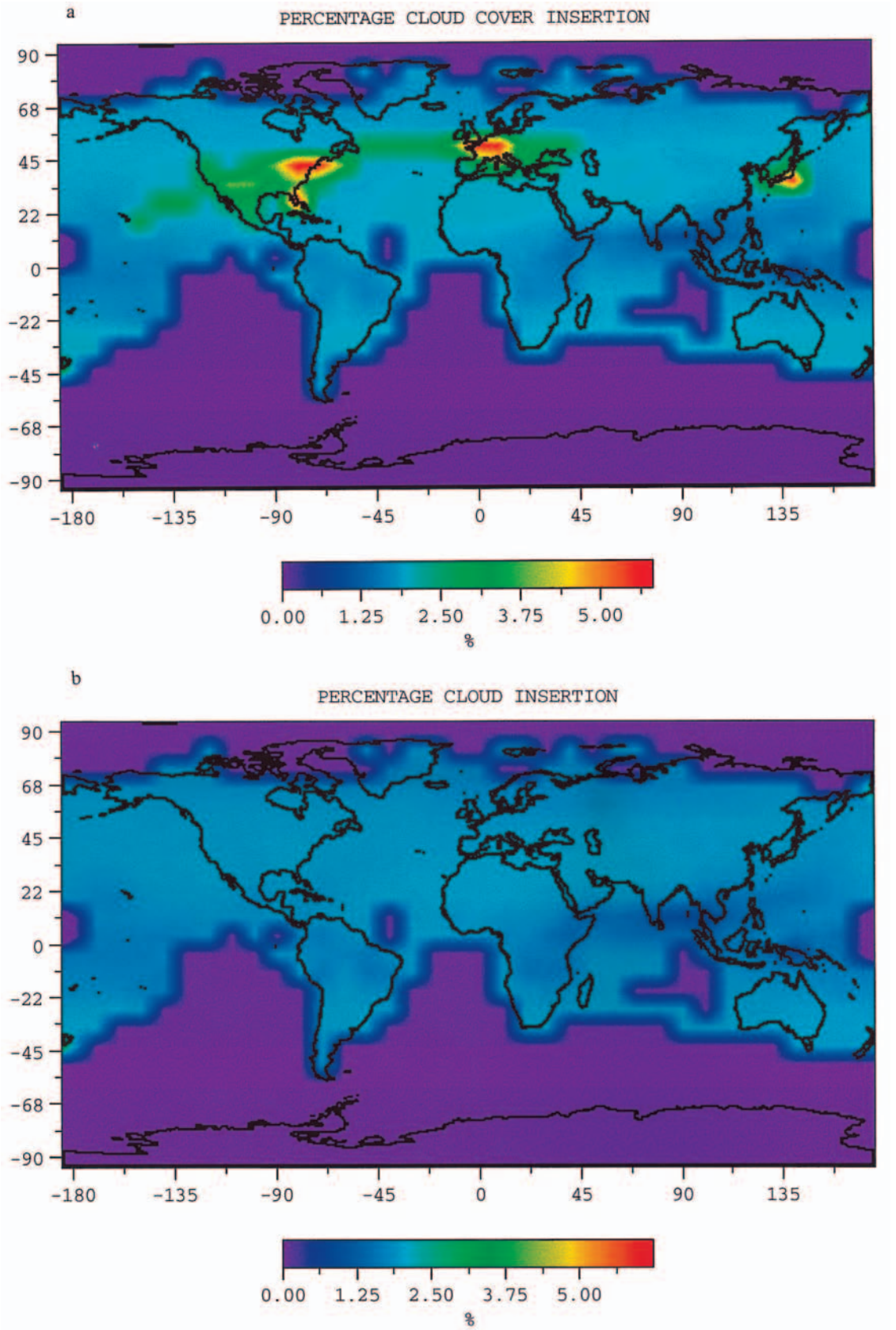

Plate 1. Percentage cloud cover insertion in several experiments. In Plate 1a cloud insertion is scaled by flight path density ("scaled" experiment); in Plate 1b it is uniform with flight path occurrence (experiment 1/99). Results are averaged over the last five years.

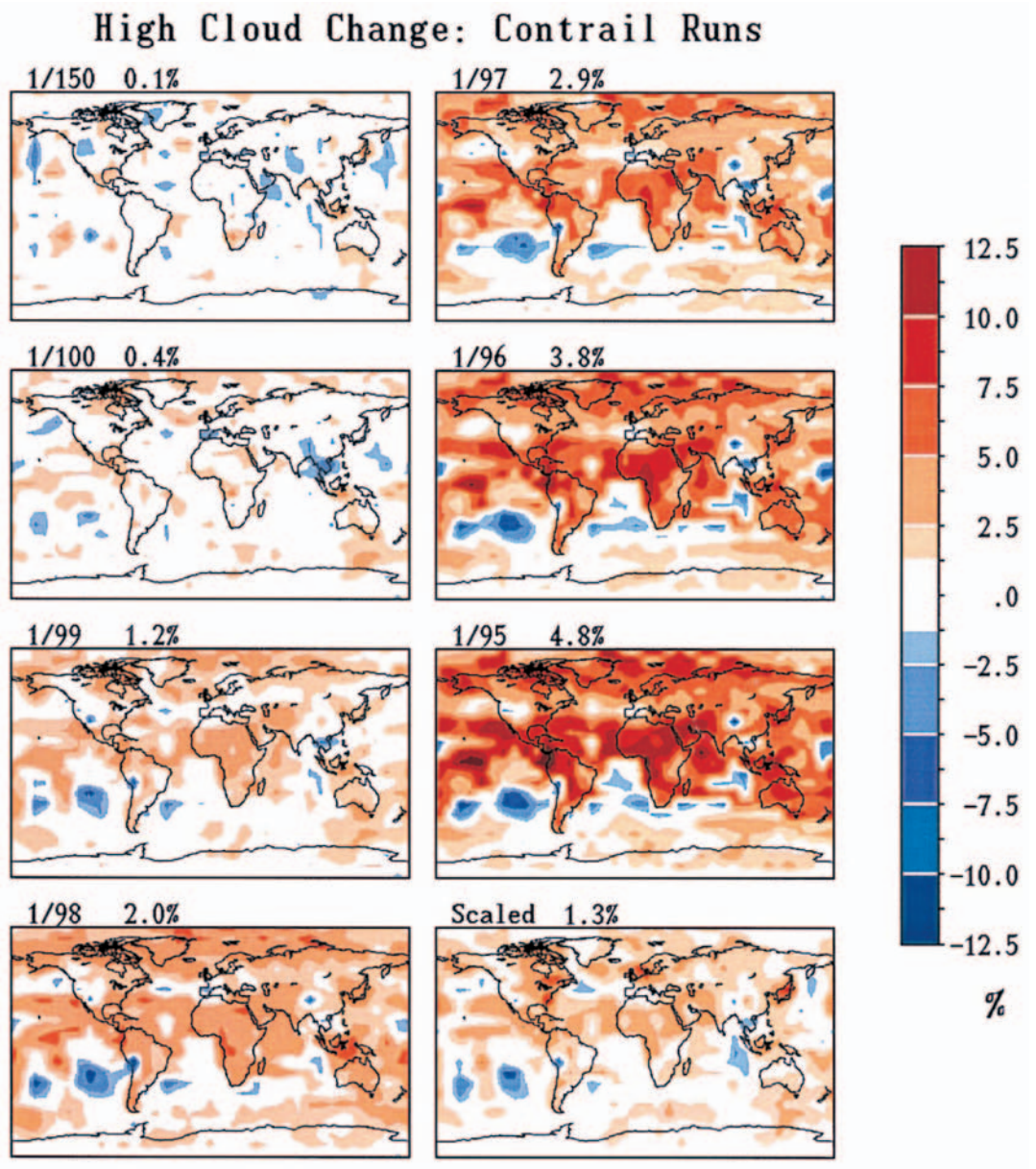

Plate 2. Absolute percentage of high-level cloud cover changes in the different experiments relative to the control run. The number in each top left-hand corner indicates the clear-sky occurrences after which the first cloud is inserted; the percentage in each center refers to the total impact on upper level cloud cover. Results in this and other figures are averages over the last 30 years of 50 year experiments.

3.2. Temperature

The latitudinal distribution of the annual surface air temperature change is shown in Figure 2. With the smaller inputs, the response is relatively uniform from 10°S to 60°N; at the greater inputs, there is more amplification in the tropics and high latitudes. The tropical response is the result of amplified high-level cloud cover (and water vapor) feedbacks, as evident in Plate 2. With increased warming, there is increased moist convection at low latitudes and also some amplification of the Hadley circulation. Greater upward motion in the tropics leads to increased high-level moisture and cloud cover. The amplified Hadley cell also results in greater subsidence in the subtropics, which helps explain the tendency for a minimal high-level cloud cover increase at those latitudes in Plate 2 (and actual cloud cover decrease in the 500–200 mbar level from the subtropics through lower middle latitudes).

The high-latitude amplification is associated with both increased high-level clouds (e.g., Plate 2) and decreased sea ice. The sea ice reduction in the Southern Hemisphere is actually greater than in the Northern Hemisphere in these experiments, by a factor of 2 or more. Nevertheless, without the high-level cloud cover increase, the Southern Hemisphere polar warming is considerably smaller. It can also be seen that scaling the cloud input by aircraft flight density may reduce the warming slightly in the Southern Hemisphere.

The altitudinal distribution of the warming is given in Figure 3. As the warming intensifies, it more clearly peaks in the upper troposphere. This response is native to the model; it

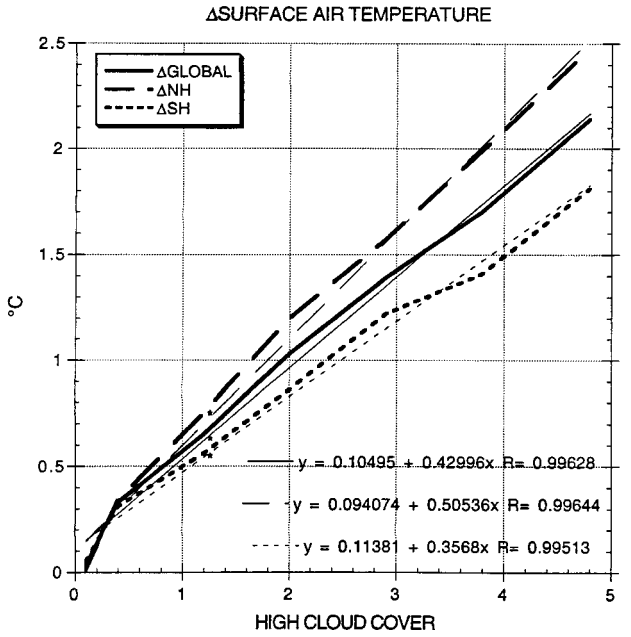

Figure 1. Annual surface air temperature change as a function of upper level cloud cover change. The thin lines represent the linear fit. The asterisks are the results of the experiment with scaled cloud input.

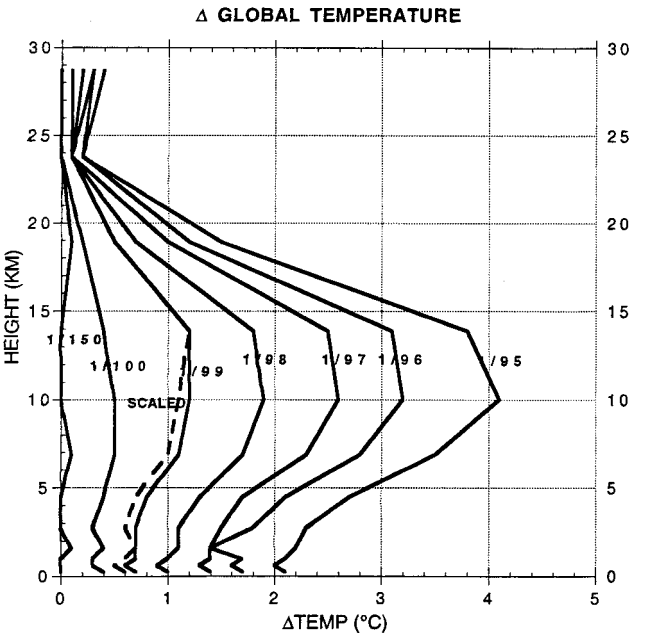

Figure 3. Global average temperature change as a function of altitude.

occurs with doubled CO_2 as well [e.g., *Rind et al*., 1998], so it is primarily a result of the cloud and water vapor feedback noted above, as opposed to the input cloud cover. When the feedbacks are minimal, in the smaller input experiment, the warming is relatively uniform with altitude (see also *Hansen et al*. [1997] for a similar result).

The geographic distribution of the surface air temperature change is given in Plate 3. Outside of the expected Northern Hemisphere bias, there is no obvious geographical bias to the warming consistent with the input fields, either for the uniform or for the scaled experiments. What is observed mostly is the feedback of the system, both radiative (with greater latent heat loss minimizing the warming over the oceans somewhat) and resultant advection patterns set up by differential heating such as that associated with the land/ocean contrast. Hence no greater geographically specific "footprint" is visible. This result contrasts with what arises when sea surface temperatures are not allowed to adjust, and the climatic response is due mostly to the radiative perturbation produced locally by the increased cloud cover [e.g., *Ponater et al*., 1996]. The system feedbacks provide much of the heating and remove evidence of the forcing distribution (as is true, for example, in solar radiation increase experiments [e.g., *Hansen et al*., 1984]).

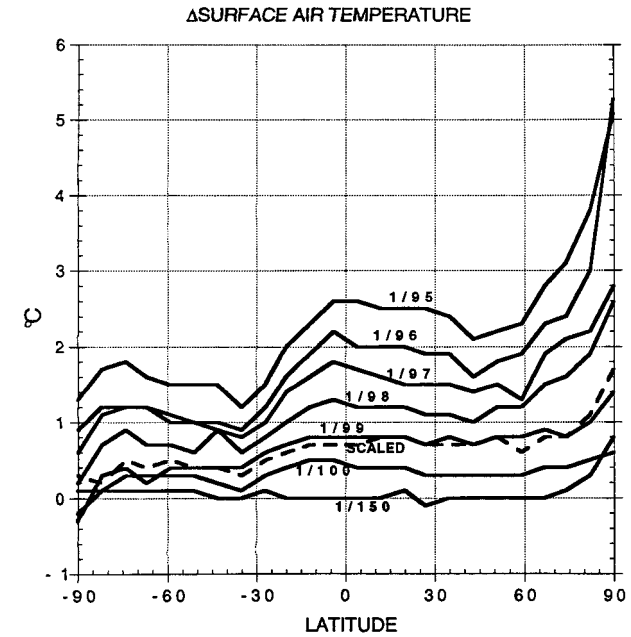

Figure 2. Surface air temperature change as a function of latitude in the different experiments. The scaled experiment results are shown by the dashed line.

Given the natural variability of the atmosphere, at what level would contrail effects such as these be observed? Plate 4 shows the ratio of the microwave signal of the model, evaluated with an off-line radiative transfer processor [*Shah and Rind*, 1995], to the standard deviation of the microwave sounding unit (MSU) observations for the experiment in which upper level clouds are altered by 0.4%. Results are shown for the different MSU channels for which standard deviations are available. Even with this small level of cirrus cloud change, a signal of more than 2 standard deviations is noticeable, especially in the stratosphere and midtroposphere channels, although its relationship to aircraft flight paths is not overly obvious. The microwave signature for the commensurate uniform and scaled cloud insertion experiments are given in Plates 5a and 5b and the signal to noise ratio in Plates 6a and 6b. The strongest signal in both experiments occurs in the upper troposphere channel 3r; at this level, in neither experiment is a detailed flight path effect obvious. The signature is somewhat different in the midtroposphere, with a slightly greater flight-path resemblance in the scaled experiment. In terms of signal to noise

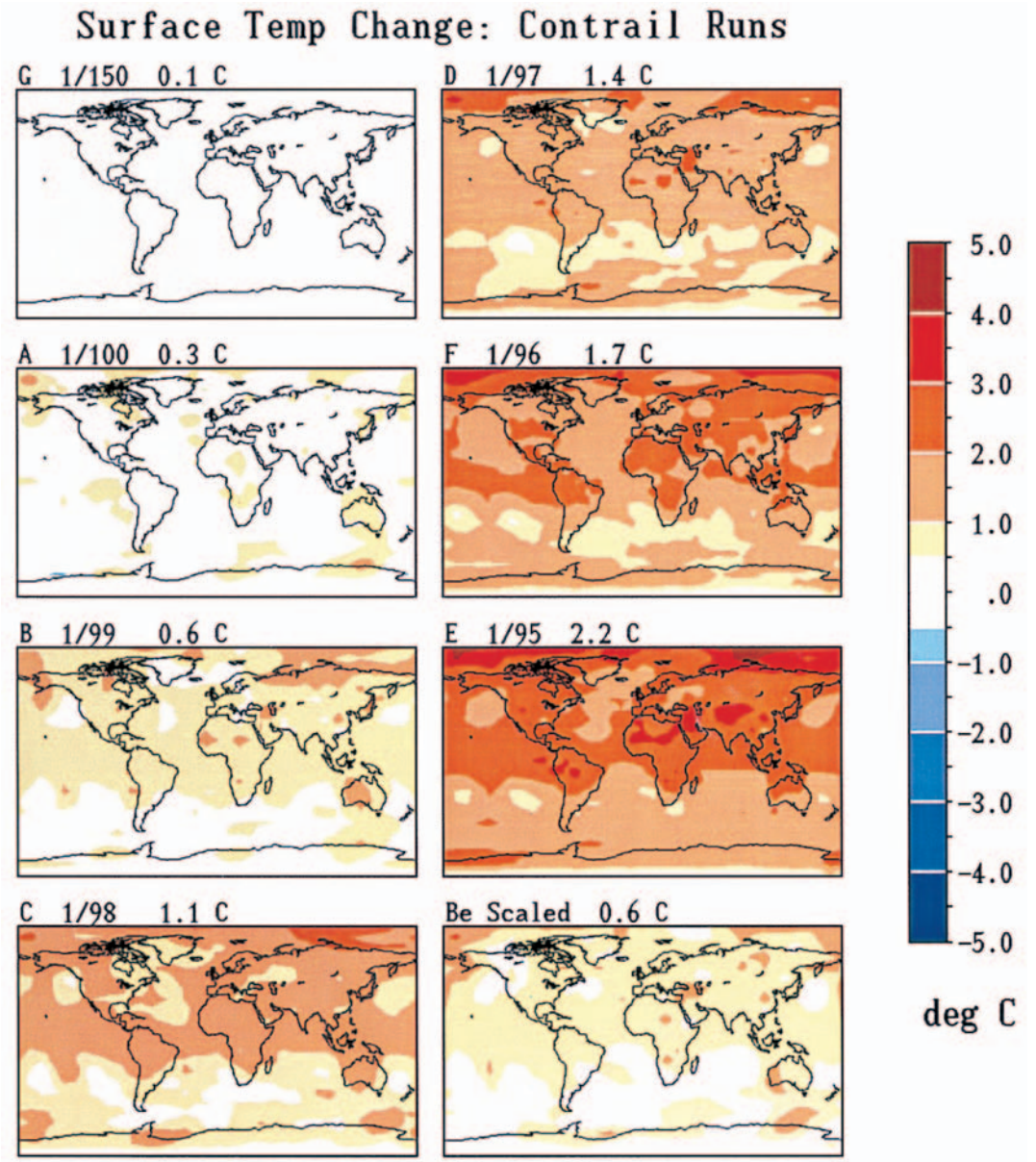

Plate 3. Surface air temperature change in the different experiments. The number in the center of each box represents the global surface air temperature change.

(Plate 6), there are many more similarities than differences between the experiments. Note that the absence of available variability statistics for the upper troposphere channel keeps us from assessing the region where the absolute signal is strongest.

3.3. Radiative Forcing

It has become standard practice to compare various climatic forcings by comparing their radiative perturbations (i.e., their "global warming potential" [*IPCC*, 1996]; this should be differentiated from their "climate sensitivity," which refers to the surface air temperature response). The addition of cirrus clouds forces a radiative perturbation, and it is of interest to see how the results in these experiments compare with those due to altered anthropogenic emissions. However, given that the input is time- and space-dependent, it is not a straightforward procedure to calculate the three-dimensional effects. As an approximation, we show in Table 2 the radiative forcing for the different experiments, averaged over the first 1 or 2 years of each experiment (2 year averages were used for the first four experiments to incorporate more input cloud cover and to provide a better estimate of the radiative forcing). True radiative forcing would be calculated without any temperature response; as shown in the table (Δsurf temp initial), the temperature response over this time period was generally small but not zero. Therefore the estimated radiative forcing is an underestimate: the warming already experienced will have increased the thermal radiation to space and hence reduced the net radiative forcing. The magnitude of the necessary correction is calculated below.

Ignoring, for the moment, this underestimate, we can first ask whether the climate sensitivity from cirrus cloud introduction is the same as that for well-mixed gases in the troposphere. The sensitivity of the model for climate perturbations due to

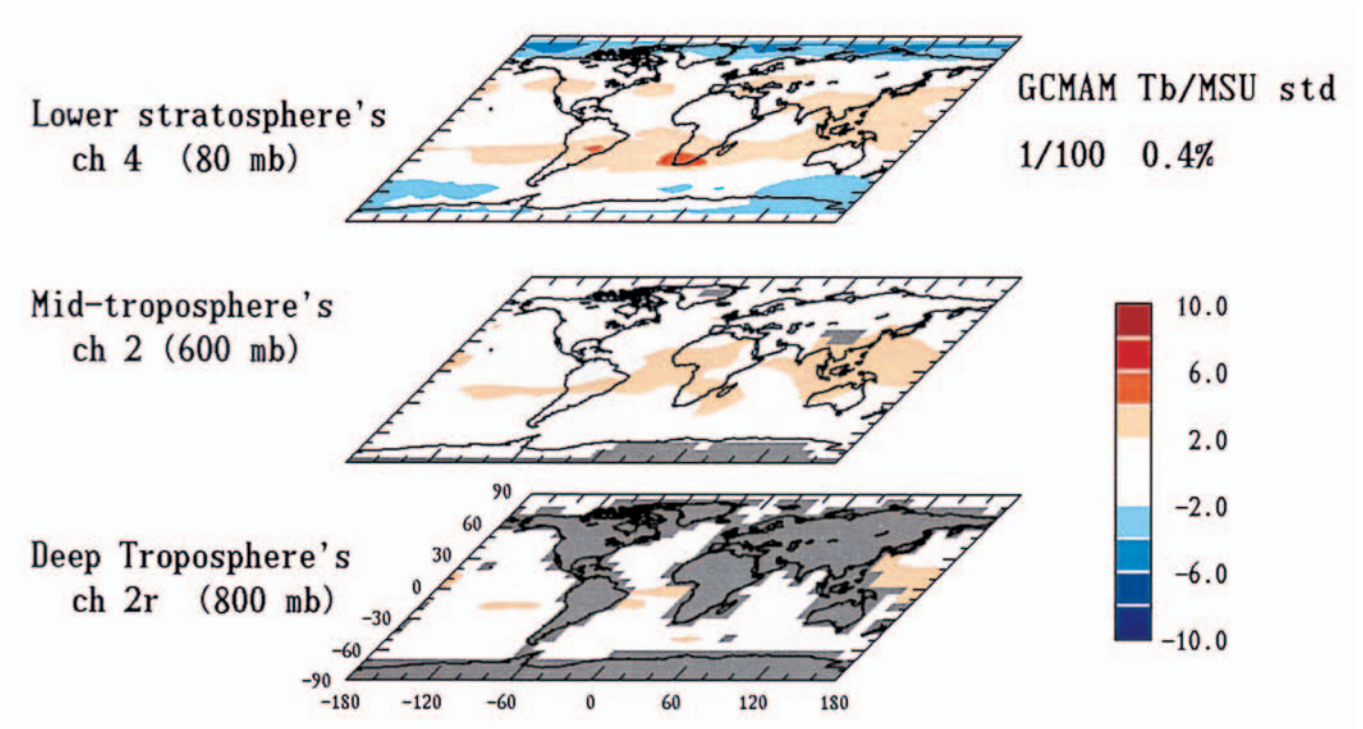

Plate 4. Ratio of the microwave brightness temperature changes in the different microwave sounding unit (MSU) channels divided by the standard deviation of the MSU observations for experiment 1/100.

well-mixed gases in equilibrium is ~1.2°C W m^{-2}. Comparing the surface air temperature response to the initial radiative forcing at the tropopause for the more extreme experiments produces a roughly similar value. Therefore using this approximate value and assuming linearity for the range of experiments, we can correct the radiation imbalance for the initial temperature warming. For example, for the 4.8% high cloud increase experiment, the net radiative forcing should be a few tenths W m^{-2} greater, associated with the warming of a few tenths °K that occurred during the first year. The corrected values are shown in parentheses in Table 2. With this correction the climate sensitivity for cirrus cloud input in these locations is closer to 0.9°C W m^{-2}. Therefore the sensitivity of the modeled system to cirrus cloud enhancements along aircraft flight paths is similar to, although perhaps slightly lower than, its sensitivity to well-mixed gases (or solar irradiance variations, which in this model produce a similar sensitivity compared to altered CO_2 [*Hansen et al.*, 1984]).

As indicated in Table 2, the clear-sky radiation actually becomes more negative. In clear-sky regions, solar radiation is reflected less than in cloudy regions and produces a positive radiative forcing for the climate system. Therefore the presence of clouds makes the net radiation at the tropopause or at the top of the atmosphere more negative. As clouds are now occurring in areas that were previously clear, the area of clear sky is less, hence there is less area for the positive radiative forcing to occur. The effect is close to proportional to the cloud cover change. For example, in the control run, the net clear-sky radiation at the tropopause is close to 23 W m^{-2}. A 5% increase in high cloud cover, as occurred for the most extreme experiment, reduced this value by 1.1 W m^{-2}, close to a 5% effect. A 3% increase in cloud cover, as was the approximate change in experiment 1/97, produced a clear-sky radiative decrease of 0.7 W m^{-2}, an ~3% effect.

4. Discussion

The experiments discussed here illustrate the extreme sensitivity of the modeled climate system to cirrus cloud cover variations. As shown above, a 1% change in cloud cover results in a 0.4°K change in global surface air temperature. With the uncertainty in high-level cloud cover observations from different techniques [e.g., *Mazin et al.*, 1993; *Liao et al.*, 1997], it is doubtful such a change would be detectable. We note that the radiative forcing calculated here for a 0.1% change in upper level cloud cover, of 0.01 W m^{-2}, is close to the value estimated from radiative transfer calculations and Earth Radiation Budget Experiment measurements [*Hartmann et al.*, 1992] (of 0.02 W m^{-2}), despite the differing locations of aircraft-induced and naturally occurring cirrus. The GCMs climate sensitivity is at the high end of the estimate from *IPCC* [1996], and so the surface temperature response to this radiative forcing may be somewhat lower in other models.

The relevance of this calculation to actual contrail radiative forcing is difficult to estimate. Many simplifications have been employed which could affect the result. Most obvious is the lack of relationship to relative humidity in the technique utilized, which means some of the high-level clouds were input at times when the region was very dry. This would exaggerate the radiative forcing, for it provides greenhouse capability where relatively little was available previously.

In addition, no seasonal or diurnal variation of contrail input was employed. Several observations have indicated a greater likelihood of contrails during winter or spring, with a minimum

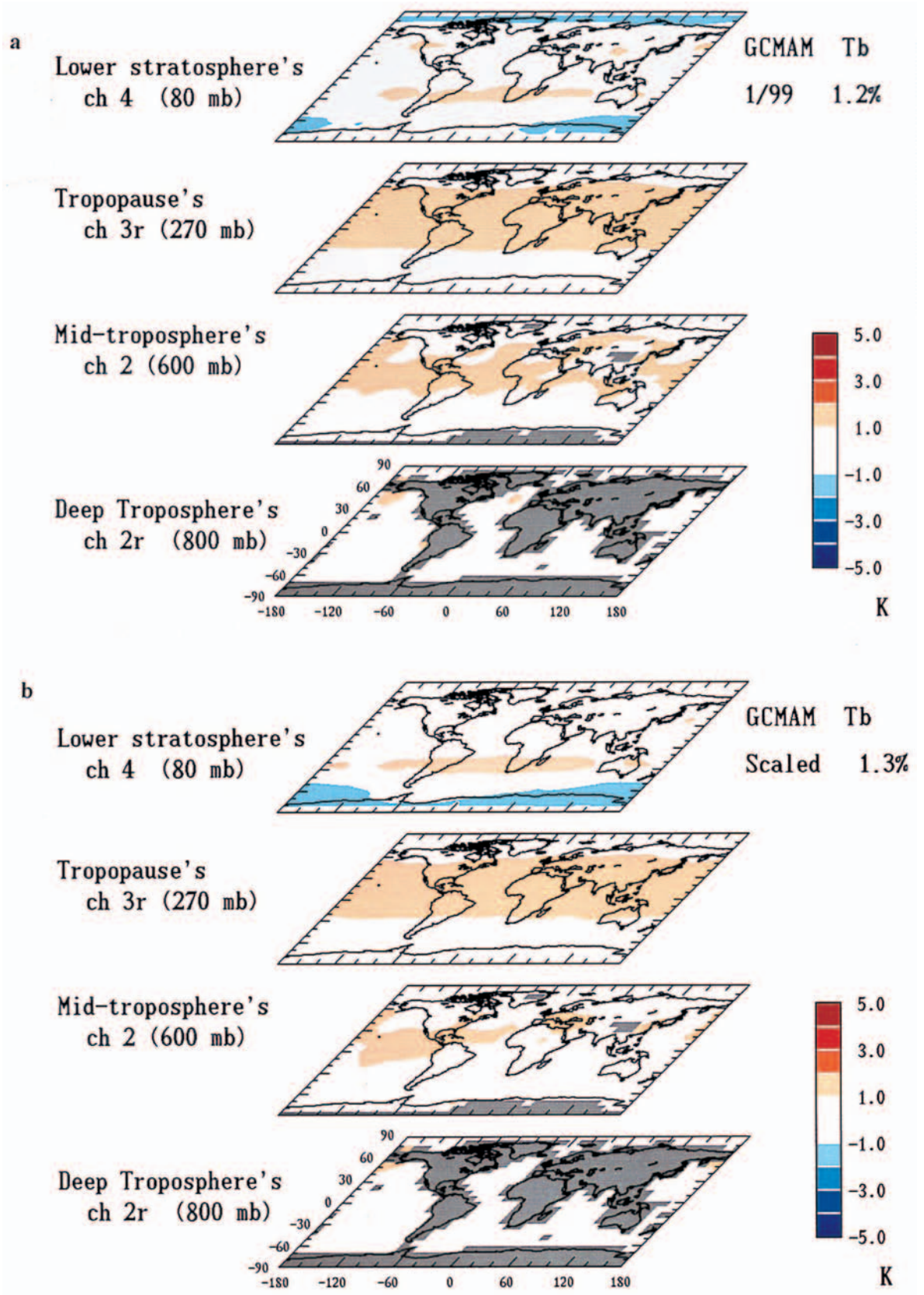

Plate 5. Microwave brightness temperature changes in the MSU channels for (a) experiment 1/99 and (b) the scaled-cloud input experiment.

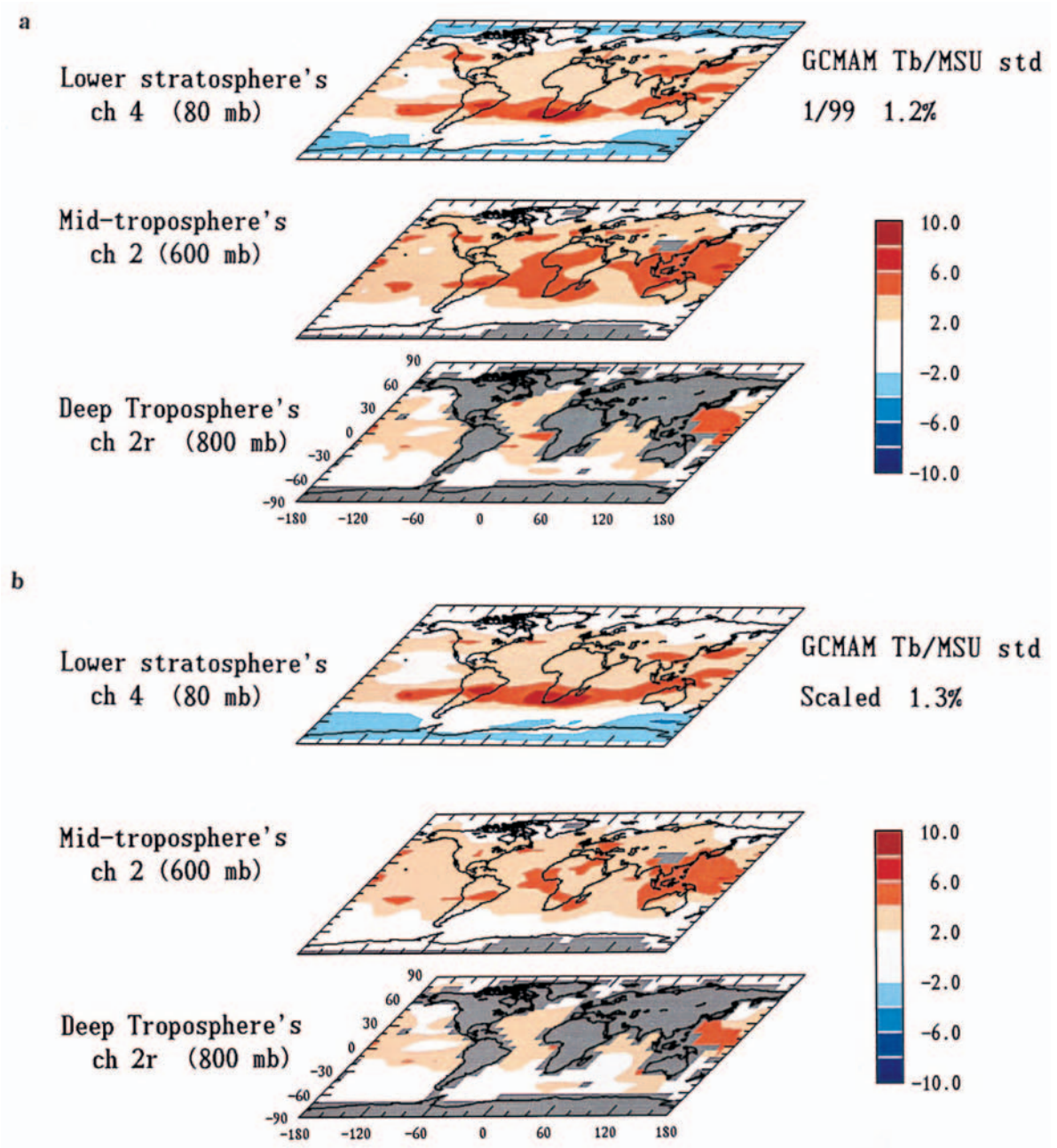

Plate 6. (a, b) As in Plates 5a and 5b except for the temperature change normalized by MSU standard deviations.

in summer [*Minnis et al*., 1997; *Sassen*, 1997; *Mannstein et al*., 1999]. By inputting cirrus without regard to season (hence underestimating the winter input), we amplify the radiative forcing (which would be smaller in winter with cold surface temperatures in the extratropics) but diminish the surface air temperature response to the forcing (which is largest in winter due to the increased atmospheric stability and sea ice/snow cover feedbacks).

The prescription also did not differentiate between day and night. Observations indicate a day/night ratio of 2–3 in contrail occurrence [*Bakan et al*., 1994; *Mannstein*, 1997]. At night the total radiative effect consists only of the longwave greenhouse warming, without the minimizing influence of solar radiation reflection, so a random prescription overemphasizes this effect. This factor is offset to some extent by the reduced greenhouse forcing associated with the colder surface air temperatures at night.

With the results as given, what does this mean for contrail impacts on climate? In the introduction it was noted that aircraft cirrus cloud radiative forcing is probably of the order of 0.04 W m^{-2} associated with an upper level cloud cover increase of 0.2%. Higher values are however possible, as there is the persistent impression that aircraft effects may well be underestimated by the attribution method (of linear contrails) and the difficulty in determining associated impacts to natural cirrus. The first two experiments listed in Table 2 therefore probably bound the effect, both in terms of impacts on cirrus as well as radiative forcing. Using the relationship shown in Fig-

Table 2. Global Changes in Radiative Forcing and Surface Temperature Response

Experiment	ΔHigh Cloud Cover, %	ΔNet Rad at Top, W m^{-2}	ΔNet Rad at Trop, W m^{-2}	ΔNet Clear-Sky at Top, W m^{-2}	ΔNet Clear-Sky at Trop, W m^{-2}	ΔSurf Temp Initial, °C	ΔSurf Temp (Equil), °C
1/150	0.1	−0.1	0 (0.01)	0.1	0.1	0.01	0.1
1/100	0.4	0	0.1 (0.19)	−0.3	−0.3	0.09	0.3
1/99	1.2	0.2	0.4 (0.49)	−0.5	−0.5	0.09	0.6
Scaled	1.3	0	0.2 (0.18)	−0.6	−0.5	−0.02	0.6
1/98	2*	0.6	0.8 (0.93)	−0.8	−0.7	0.13	1.1
1/97	2.9*	0.9	1.2 (1.4)	−0.8	−0.7	0.21	1.4
1/96	3.8*	1.3	1.8 (2.0)	−1.2	−1.0	0.23	1.7
1/95	4.8*	1.6	2.2 (2.4)	−1.4	−1.1	0.25	2.2

Values corrected for the initial temperature change are given in parentheses. Net radiation values are indicated at the top of the model and at the tropopause (Trop).

*Using first year data, otherwise average of first 2 years.

ure 1 would imply a current, equilibrium impact of 0.086°C; since the jet era began only 30 years ago, not long enough to achieve equilibrium, and the current coverage is larger than the average over this time period, that value would represent an upper bound of this aircraft cirrus cloud and surface temperature effect. If one assumes that the observed cirrus change of 0.3% since the 1960s is all due to aircraft, the equilibrium response would be some 0.13°C, again not all of which would have been achieved. As noted above, with a 0.4% impact on cloud cover, a significant response is observable in MSU observations (at equilibrium).

Considering the estimates for 2050, assuming a factor of 3.2 increase in aviation fuel consumption relative to 1992 (a factor of 4.3 above 500 mbar), *IPCC* [1999] estimated the likelihood of a factor of 5 increase in aircraft impact on linear persistent contrails relative to today, with a factor of 4 increase in overall cirrus impact (depending on fuel use scenarios, efficiencies, and spatial distribution of future traffic). A 2050 estimate of close to 0.4% coverage increase would result in a global temperature change, as in the 1/100 experiment, of close to 0.3°C. An extreme estimate, resulting from a factor of 14 increase in fuel consumption, would be 1–2% increase in coverage, which would then force surface temperature changes of 0.45°–0.9°C, as shown in the 1/99 and 1/98 experiments in Table 2. This magnitude would be a significant addition to any assumed anthropogenic climate change by 2050, estimated to be of the order of 1°–2°C due to CO_2 and other trace gas releases [*IPCC*, 1996] (although this value would be higher in equilibrium).

How does the radiative forcing calculated in these experiments compare with that due to estimated anthropogenically induced changes during the next century? As indicated in *IPCC* [1995], total radiative forcing, following the IS92a scenario, is expected to be of the order of 3.5 W m^{-2} by 2050; if one considers the non-CO_2 trace gases, it is slightly more than 2 W m^{-2}. This value is close to the radiative forcing associated with the most extreme of these experiments and is produced by altering the high-level cloud cover by a little less than 5%. Therefore if aircraft alter upper level cirrus more than is currently anticipated (or observed), it could have a highly significant impact on the climate of the next century.

As shown in Figure 2, a major distinction between climate change associated with well-mixed gases and that generated in these experiments is the hemispheric differentiation of both the forcing and the response. Given in Tables 3a and 3b are the high cloud cover changes, radiative forcing, and surface air temperature responses in the two hemispheres for the different experiments. It is apparent that the initial radiative forcing is considerably larger in the Northern Hemisphere, as is the initial surface air temperature response. The equilibrium responses, while still greater in the Northern Hemisphere, are not so different. A question in this regard is: how does the Southern Hemisphere warm, by transport of heat from the Northern Hemisphere, or in situ radiative forcing changes, due to feedbacks within its own hemisphere?

Table 4a shows estimates of the contributions to warming in the most extreme of the cloud cover input experiments (1/95), for the global average and the two hemispheres. The results come from comparison of present results to previous analysis of the sensitivity of this model to the various feedbacks, both with a one-dimensional (1-D) radiative-convective model [*Hansen et al*., 1984] and a 2-D analysis [*Pollack et al*., 1993]. Given the approximate nature of the technique, uncertainties of the order of 10% are probable, as estimated by the difference between the total estimated warming and the actual

Table 3a. Northern Hemisphere Changes in Radiative Forcing at Top of the Atmosphere and the Tropopause (Trop), and Surface Temperature Response

Experiment	ΔHigh Cloud Cover, %	ΔNet Rad at Top, W m^{-2}	ΔNet Rad at Trop, W m^{-2}	ΔNet Clear-Sky at Top, W m^{-2}	ΔNet Clear-Sky at Trop, W m^{-2}	ΔSurf Temp Initial, °C	ΔSurf Temp (Equil), °C
1/150	0.08	0.5	0.6	0.2	0.3	0.07	0.01
1/100	0.41	−0.1	0.2	−0.6	−0.5	0.20	0.34
1/99	1.3	0.9	1.0	−0.6	−0.4	0.16	0.75
Scaled	1.65	0.8	1.2	−0.5	−0.4	0.07	0.73
1/98	2.20	1.0	1.4	−1.0	−0.9	0.26	1.20
1/97	3.3	1.3	2.0	−1.1	−1.0	0.33	1.57
1/96	4.4	2.3	3.2	−1.6	−1.3	0.34	1.99
1/95	5.7	2.8	3.7	−1.4	−1.2	0.43	2.48

Table 3b. As in Table 3a for the Southern Hemisphere

Experiment	ΔHigh Cloud Cover, %	ΔNet Rad at Top, W m^{-2}	ΔNet Rad at Trop, W m^{-2}	ΔNet Clear-Sky at Top, W m^{-2}	ΔNet Clear-Sky at Trop, W m^{-2}	ΔSurf Temp Initial, °C	ΔSurf Temp (Equil), °C
1/150	0.12	−0.6	−0.7	0	0	−0.05	0.05
1/100	0.39	0.1	0	0.1	0	−0.01	0.31
1/99	1.1	−0.4	−0.2	−0.5	−0.4	0.01	0.56
Scaled	0.95	−0.8	−0.8	−0.7	−0.6	−0.11	0.51
1/98	1.79	0.1	0.1	−0.6	−0.5	0	0.86
1/97	2.5	0.3	0.3	−0.5	−0.4	0.09	1.22
1/96	3.2	0.1	0.2	−0.8	−0.7	0.13	1.41
1/95	3.8	0.3	0.5	−1.2	−1.1	0.08	1.81

warming for this experiment (Table 3; the actual warming is repeated in parentheses in the last row). It can be seen that the Southern Hemisphere warming is primarily the result of the cloud cover height changes, with the obvious high cloud cover increase, and a low-level cloud cover decrease (of the order of 1%). The high cloud cover increase is 50% greater in the Northern Hemisphere, as is the estimated associated warming. The water vapor response is only slightly higher in the Northern Hemisphere, due most likely to its greater warming. The planetary albedo increase provides a negative forcing. While the ground albedo actually decreased (by 0.36% in the Northern Hemisphere and 0.12% in the Southern Hemisphere) due to less snow and sea ice, the increase in high-level cloud cover increased the atmospheric albedo sufficiently to provide greater overall reflection. In comparison, increased moist static energy transport across the equator cools the Northern Hemisphere and warms the Southern Hemisphere only slightly.

How does this result compare with that from the well-mixed greenhouse gas forcing? Table 4a also shows the results from a doubled CO_2 experiment with the same model [*Rind et al*., 1998] (initial radiative forcing of 4.3 W m^{-2} at the top of the atmosphere, 4.6 W m^{-2} at the tropopause). As is obvious, the hemispheric distribution of warming is more equally distributed. The high cloud cover forcing is now somewhat greater in the Southern Hemisphere than in the Northern Hemisphere, as is the water vapor feedback and the planetary albedo change (associated with both greater sea ice decrease and greater low-level cloud cover decrease). As high-level cloud cover change is smaller (amounting to a global average of 1.7%, 3% in the Southern Hemisphere and only 0.5% in the Northern Hemisphere), it does not offset the other albedo changes, and the planetary albedo forcing provides additional warming. As expected therefore, distinct hemispheric differences arise in equilibrium responses to high cloud (greenhouse-type) forcing occurring primarily in the Northern Hemisphere versus the well-mixed greenhouse gas forcing.

Clearly, the ratio of the global water vapor feedback to the cloud height feedback is greater in the doubled CO_2 experiment than in the cloud insertion experiment. How does this change with the magnitude of the warming, which is larger with doubled CO_2? In Table 4b we show the same values for the experiment that altered high-level cloud cover by 1.2% and resulted in considerably less warming. The ratio of the global cloud-height-induced warming to the water-vapor-induced warming in that experiment (2.2) is essentially the same as that in the most extreme experiment shown in Table 4a (a ratio of 2.13). It appears therefore that the cloud height feedback will dominate the water vapor feedback in this type of experiment over a range of warming values, an effect that occurs in both hemispheres.

Finally, we can compare this last experiment with its scaled equivalent, in which cloud insertion was made proportional to the density of flight paths through the region. As shown in Table 4b, the cloud height effect is more greatly emphasized in the Northern Hemisphere compared to the Southern Hemisphere in the scaled experiment, consistent with the greater Northern Hemisphere peak insertions. As compensation, the water vapor response actually is greater in the Southern Hemisphere in the scaled experiment, helped perhaps by the slightly larger energy transport across the equator. The overall equilibrium warming in the two hemispheres is within 10% between the two experiments.

5. Conclusions

The insertion of cirrus cloud cover along flight paths in the Northern Hemisphere has a noticeable impact on climate. The sensitivity in the model used here is such that a 1% change in

Table 4a. Equilibrium Temperature Change (°C) Estimates Due to Feedbacks and Transport (Trans) in Different Climate Change Experiments

	High Cloud Cover Insertion (1/95)			$2 \times CO_2$		
	Global	NH	SH	Global	NH	SH
$2 \times CO_2$	NA	NA	NA	1.2	1.2	1.2
ΔH_2O	0.75	0.8	0.7	1.6	1.5	1.7
ΔPlan albedo	−0.2	−0.3	−0.1	0.9	0.75	1.05
ΔCloud height	1.6	1.9	1.3	1.4	1.1	1.7
ΔTrans	NA	−0.1	0.1	NA	0.5	−0.5
Total	2.15 (2.2)	2.3 (2.5)	2.0 (1.8)	5.1 (5.1)	5.05 (5.0)	5.15 (5.1)

Actual temperature changes are shown in parentheses.

Table 4b. As in Table 4a for the Equivalent Unscaled and Scaled Cloud Insertion Experiments

	Unscaled Experiment (1/99)			Scaled Experiment		
	Global	NH	SH	Global	NH	SH
ΔH_2O	0.15	0.23	0.08	0.20	0.23	0.18
ΔPlan albedo	0.04	0.08	0	−0.055	−0.07	−0.04
ΔCloud height	0.40	0.43	0.38	0.44	0.55	0.33
ΔTrans	NA	−0.02	0.02	NA	−0.05	0.05
Total	0.60 (0.6)	0.72 (0.75)	0.48 (0.56)	0.59 (0.6)	0.66 (0.73)	0.52 (0.51)

cloud cover gives rise to a global warming of some 0.4°C. The warming is greater in the Northern Hemisphere and as such differs from that associated with uniform trace gas releases in this model. The surface warming peaks at the highest northern latitudes, and on the global average in the upper troposphere. Longitudinally, the land/ocean contrast in warming plays a bigger role than the flight path distribution. In this regard, results are similar regardless of whether the cloud insertion is made proportional to flight path density, or simply associated with flight path occurrence.

Significant warming in tropospheric temperatures (relative to MSU natural variability) occurs with an impact on upper level cloud cover of 0.4% (with a radiative forcing at the tropopause of about 0.1 W m^{-2}). This can be compared to estimates of the current aircraft impact on cirrus clouds of 0–0.2% and radiative forcing of 0–0.08 W m^{-2}. It would seem as if a slight increase in current day values (assuming the estimate of the current influence is correct) would thus be sufficient to produce a noticeable equilibrium effect, at least with the sensitivity to that perturbation which occurs in this GCM. Estimates for 2050 of radiative forcing from 0.03 to 0.4 W m^{-2} may therefore lead to a significant impact; the radiative forcing of 0.4 W m^{-2} at the tropopause produced an equilibrium surface air temperature warming of 0.6°C.

Not surprisingly, the equilibrium warming was dominated by the change in cloud height, as compared to a doubled CO_2 experiment with the same model in which the water vapor feedback was somewhat more important. In these experiments we did not change the optical thickness of cirrus clouds, in line with observations that persistent contrails become indistinguishable from natural cirrus. The influence of aircraft water vapor release on natural cirrus is hard to estimate; in experiments done with this model, the water vapor release was sufficiently small when averaged over a grid box that no effect was noticeable [*Rind et al*., 1996]. Aircraft sulfur and soot releases, as well as metal contaminants, may influence the number of ice condensation nuclei and thus particle size and concentration. Were aircraft to double the optical thickness of cirrus clouds, this would maximize the difference between their greenhouse warming potential and their reflectivity and exacerbate their impact on surface temperatures. Conversely, smaller more numerous particles would probably increase their albedo and reduce warming. Additional observations will be required to understand this aspect of potential aircraft influence on the climate system as well as help quantify how much aircraft really are changing upper level cloud cover.

Acknowledgments. This work was supported by a NASA grant under the AEAP, SASS program. GCMAM modeling is supported by the ACMAP program.

References

Bakan, S., M. Betancor, V. Gayler, and H. Grassl, Contrail frequency over Europe from NOAA-satellite images, *Ann. Geophys*., *12*, 962–968, 1994.

Boucher, O., Air traffic may increase cirrus cloudiness, *Nature*, *397*, 30–31, 1999.

Brewer, A. W., Condensation trails, *Weather*, *1*, 34–40, 1946.

Gierens, K., R. Sausen, and U. Schumann, A diagnostic study of the global distribution of contrails, part II, Future air traffic scenarios, *Theor. Appl. Climatol*., *63*, 1–9, 1999.

Hansen, J., G. Russell, D. Rind, P. Stone, A. Lacis, S. Lebedeff, R. Ruedy, and L. Travis, Efficient three dimensional global models for climate studies: Models I and II, *Mon. Weather Rev*., *111*, 609–662, 1983.

Hansen, J., A. Lacis, D. Rind, G. Russell, P. Stone, I. Fung, R. Ruedy, and J. Lerner, Climate sensitivity: Analysis of feedback mechanisms, in *Climate Processes and Climate Sensitivity*, edited by J. Hansen and T. Takahashi, pp. 130–163, *Geophys. Monogr*., vol. 29, AGU, Washington, D. C., 1984.

Hansen, J. E., M. Sato, and R. Ruedy, Radiative forcing and climate response, *J. Geophys. Res*., *102*, 6831–6864, 1997.

Hartmann, D. L., M. E. Ockert-Bell, and M. L. Michelsen, The effect of cloud type on earth's energy balance: Global analysis, *J. Clim*., *5*, 1281–1304, 1992.

Heymsfield, A. J., L. M. Miloshevich, C. Twohy, G. Sachse, and S. Oltmans, Upper tropospheric relative humidity observations and implications for cirrus ice nucleation, *Geophys. Res. Lett*., *25*, 1343–1346, 1998.

International Panel on Climate Change (IPCC), *Climate Change 1995—The Science of Climate Change*, edited by J. H. Houghton, L. G. Meira Filho, B. A. Callander, N. Harris, A. Kattenberg, and K. Maskell, 572 pp., Cambridge Univ. Press, New York, 1996.

IPCC, *Aviation and the Global Atmosphere*, edited by J. E. Penner, D. H. Lister, D. J. Griggs, D. J. Dokken, and M. McFarland, 370 pp., Cambridge Univ. Press, New York, 1999.

Jager, H., V. Freudenthaler, and F. Homburg, Remote sensing of optical depth of aerosols and cloud cover related to air traffic, *Atmos. Environ*., *32*, 3123–3127, 1998.

Knollenberg, R. G., Measurements of the growth of ice budget in a persisting contrail, *J. Atmos. Sci*., *29*, 1367–1374, 1972.

Liao, X., W. B. Rossow, and D. Rind, Comparison between SAGE II and ISCCP high-level clouds, part I, Global and zonal mean cloud amounts, *J. Geophys. Res*., *100*, 1121–1136, 1995.

Mannstein, H., Contrail observations from space using NOAA-AVHRR data, in *Proceedings of the International Colloquium on the Impact of Aircraft upon the Atmosphere*, vol. II, pp. 427–431, Off. Natl. d'Etud. et de Rech. Aerosp., Chatillon, France, 1997.

Mannstein, H., R. Meyer, and P. Wendling, Operational detection of contrails from NOAA-AVHRR-data, *Int. J. Remote Sens*., *20*, 1641, 1999.

Mazin, I. P., Aircraft condensation trails, *Izv. Atmos. Oceanic Phys*., *32*, 1–13, 1996.

Mazin, I. P., S. N. Burkovskaya, and E. T. Ivanova, On the climatology of upper-layer clouds, *J. Clim*., *9*, 1812–1821, 1993.

Minnis, P. J., J. K. Ayers, and S. P. Weaver, Surface-based observations of contrail occurrence frequency over the U.S., April 1993–April 1994, *NASA Ref. Publ. 1404*, Natl. Aeronaut. and Space Admin., 1997.

Pollack, J., D. Rind, A. Lacis, J. E. Hansen, M. Sato and R. Ruedy, GCM simulations of volcanic aerosol forcing, part I, Climate

changes induced by steady-state perturbations, *J. Clim*., *10*, 1719–1742, 1993.

Ponater, M., S. Brinkop, R. Sausen, and U. Schumann, Simulating the global atmospheric response to aircraft water vapour emissions and contrails: A first approach using a GCM, *Ann. Geophys*., *14*, 941–960, 1996.

Rind, D., R. Suozzo, N. K. Balachandran, A. Lacis, and G. L. Russell, The GISS Global Climate/Middle Atmosphere Model, part I, Model structure and climatology, *J. Atmos. Sci*., *45*, 329–370, 1988.

Rind, D., P. Lonergan, and K. Shah, Climatic effect of water vapor release in the upper troposphere, *J. Geophys. Res*., *101*, 29,395–29,405, 1996.

Rind, D., D. Shindell, P. Lonergan, and N. K. Balachandran, Climate change and the middle atmosphere, part III, The doubled CO_2 climate revisited, *J. Clim*., *11*, 876–894, 1998.

Sassen, K., Contrail-cirrus and their potential for regional climate change, *Bull. Am. Meteorol. Soc*., *78*, 1885–1903, 1997.

Sausen, R., K. Gierens, M. Ponater, and U. Schumann, A diagnostic study of the global distribution of contrails, part I, Present day climate, *Theor. Appl. Climatol*., *61*, 127–141, 1998.

Shah, K., and D. Rind, Use of microwave brightness temperatures with a GCM, *J. Geophys. Res*., *100*, 13,841–13,874, 1995.

Travis, D. J., and S. A. Changnon, Evidence of jet contrail influences on regional-scale diurnal temperature range, *J. Weather Mod*., *29*, 74–83, 1997.

P. Lonergan, Science Systems and Applications, Inc., New York, NY 10025.

D. Rind, NASA Goddard Institute for Space Studies, 2880 Broadway, New York, NY 10025. (drind@giss.nasa.gov)

K. Shah, Center for Climate System Research, Columbia University, NY 10025.

(Received May 7, 1999; revised November 9, 1999;
accepted November 17, 1999.)